IEEE Access
Multidisciplinary | Rapid Review | Open Access Journal

Received February 20, 2020, accepted March 17, 2020, date of publication March 19, 2020, date of current version March 30, 2020.

Digital Object Identifier 10.1109/ACCESS.2020.2982088

OFDM With Hybrid Number and Index Modulation

AHMAD M. JARADAT[1], JEHAD M. HAMAMREH[2], AND HÜSEYIN ARSLAN[1,3], (Fellow, IEEE)
[1]Department of Electrical and Electronics Engineering, Istanbul Medipol University, 34810 Istanbul, Turkey
[2]Department of Electrical and Electronics Engineering, Antalya Bilim University, 07468 Antalya, Turkey
[3]Department of Electrical Engineering, University of South Florida, Tampa, FL 33620, USA

Corresponding author: Ahmad M. Jaradat (ajaradat@st.medipol.edu.tr)

This work was supported in part by the Scientific and Technological Research Council of Turkey (TUBITAK) under Grant 119E392.
The simulation codes used to generate the results presented in this paper can be found at https://www.researcherstore.com/.

ABSTRACT A novel transmission scheme is introduced for efficient data transmission by conveying additional information bits through jointly changing the index and number of active subcarriers within each orthogonal frequency division multiplexing (OFDM) subblock. The proposed scheme is different from the conventional OFDM-subcarrier number modulation (OFDM-SNM) and OFDM-index modulation (OFDM-IM), in which data bits are transmitted using either number or index of active subcarriers. The proposed modulation technique offers superior spectral and energy efficiency compared to its counterparts OFDM-SNM and OFDM-IM, especially at low modulation orders such as binary phase shift keying (BPSK) that can provide high reliability and low complexity, thus making it very suitable for meeting the requirements of Internet of things (IoT) applications. Bit error rate (BER) performance analysis is provided for the proposed scheme, and Monte Carlo simulations are presented to prove the consistency of the simulated BER with the analyzed one. More importantly, it is demonstrated that the proposed scheme can offer much superior BER performance compared to that of OFDM-IM and classical OFDM under equivalent power and spectral efficiency values.

INDEX TERMS OFDM, IoT, subcarriers, energy efficiency, power efficiency, OFDM-subcarrier number modulation, reliability, OFDM-HNIM, OFDM-IM, index modulation, subblock, simulation codes.

I. INTRODUCTION

5G envisions supporting a wide variety of use cases and related requirements [1], [2]. This includes satisfying conflicting goals such as reliability and latency, in addition to high data rates, improved energy efficiency, and low computational complexity targets [3], [4]. The latter two are directly impacted by the selected modulation schemes, therefore its appropriate selection for specific use cases is imperative [5]–[7].

Multicarrier transmission schemes are extensively used in wireless communications due to features, like easy equalization, multi-user scheduling and support for adaptive modulation and coding techniques, etc. [8]. The OFDM transmission scheme is arguably considered to be the most promising multicarrier techniques, leading to its widespread use in various communication standards [9]. However, the conventional OFDM scheme has certain limitations such as high peak-to-average power ratio (PAPR) [10], which necessitate improved modulation schemes, particularly for metrics such as reliability, spectral efficiency (SE), EE, etc. [7]. The diverse user requirements, such as increased capacity and massive connectivity render increased SE and EE imperative. These factors also dictate the appropriate modulation schemes, particularly for EE in mmWave bands [11].

Different OFDM-based modulation options have been proposed in the literature and their classification, comparison, and future directions have been provided in [7]. Among the promising OFDM-based modulation options, index and number based OFDM modulation schemes are attractive options, where some subcarriers are conventionally modulated, alongside the additional bits transmitted by exploiting the index or number dimension [7]. In particular, OFDM with index modulation (OFDM-IM) [12] and OFDM with subcarrier number modulation (OFDM-SNM) [13] are among the promising index-based and number-based modulation techniques for OFDM-based waveforms, respectively [7].

The OFDM-IM scheme exploits the indices of active subcarriers to transmit additional information with a fixed activation ratio per subblock, which limits the enhancement of SE.

The associate editor coordinating the review of this manuscript and approving it for publication was Donatella Darsena.

The design of the OFDM-IM codebook depends on either the look-up table procedure or the combinatorial method, which is of high complexity and has not completely exploited the frequency selectivity for reliability improvement [14]. Several improved versions of OFDM-IM schemes have been proposed in [15]–[20] with the main motivation of enhancing the SE of the conventional OFDM-IM scheme.

Among these improved OFDM-IM schemes, a generalized version of OFDM-IM known as OFDM with generalized index modulation (OFDM-GIM) has been developed [21]. OFDM-GIM is very much similar in principle to the basic OFDM-IM, where information bits are sent by indices. The only difference between these schemes is the employed policy for the determination of activation ratios throughout the OFDM block. The OFDM-IM uses only a fixed activation ratio throughout the whole OFDM block. On the other hand, OFDM-GIM employs different activation ratios per each subblock within the whole OFDM block in a deterministic, fixed manner (not random based on the incoming data). This results in changing the number of active subcarriers (but there are no bits sent by the number of subcarriers, where the information bits are still sent by indices). Moreover, the selection of the activation ratios in OFDM-GIM must be shared with the receiver so that it can perform the detection of the active subcarrier indices.

Some improved OFDM-IM schemes such as dual-mode index modulation aided OFDM (DM-OFDM) [22] and its generalized version called generalized DM-OFDM (GDM-OFDM) [23] as well as OFDM with multi-mode IM (OFDM-MMIM) [24] overcome the main limitation of OFDM-IM by transmitting data symbols on all available subcarriers along with IM. Aside from the enhancement of SE provided by these improved OFDM-IM schemes, it is difficult to mitigate intercarrier interference (ICI) and/or reduce PAPR due to activating all subcarriers.

Based on the general shape of the OFDM-IM block, a new number-based OFDM transmission scheme called OFDM-SNM is proposed in [13]. OFDM-SNM implicitly conveys information by utilizing number, instead of indices, of active subcarriers alongside the conventional symbols. An enhanced scheme of OFDM-SNM is proposed in [25], which exploits the flexibility enabled by the original OFDM-SNM scheme by placing the active subcarriers adaptively based on the channel to offer an additional coding gain in the high signal-to-noise ratio (SNR) region. The adaptation is performed based on the instantaneous channel state information (CSI), in which the incoming information bits are dynamically mapped to subcarriers with high channel power gains.

Inspired by these unique features of the OFDM-IM and OFDM-SNM schemes, we introduce a novel alternative transmission scheme called OFDM with hybrid number and index modulation (OFDM-HNIM).

Our main contributions are summarized as follows:

- We develop and propose a novel modulation scheme called OFDM-HNIM in which information bits are conveyed not only by the modulated subcarriers but also implicitly by both number and indices of active subcarriers relying on the incoming bits to embed extra information bits beside the bits conveyed by M-ary constellation symbols. Therefore, the SE is significantly improved compared to OFDM-SNM and OFDM-IM schemes while maintaining low detection complexity.
- We derive tight, closed-form expressions for upper bound on the BER of OFDM-HNIM systems assuming maximum likelihood (ML) detection. Two different ML-based detectors have been employed in the proposed OFDM-HNIM scheme: Perfect subcarrier activation pattern estimation (PSAPE), and imperfect SAP estimation (ISAPE) detectors. The log-likelihood ratio (LLR) detector is also employed with the proposed scheme to enhance the detection performance. The BER performance of the OFDM-HNIM is further compared with that of the existing state-of-the-art including OFDM-IM, OFDM-SNM, and conventional OFDM through Monte Carlo simulations.

The merits of the proposed scheme can be stated as follows:

- The proposed OFDM-HNIM scheme increases the system design flexibility by creating an extra degree of freedom in the number and index dimensions, which can be exploited for different purposes such as enhancing the overall SE of the communication system.
- Unlike conventional OFDM, DM-OFDM, and OFDM-MMIM where all subcarriers are occupied by non-zero elements, exploiting the inactive subcarriers of the proposed OFDM-HNIM scheme could be used to lessen interference among subcarriers and enhance EE by reducing PAPR. Moreover, it is possible to utilize the inherent features of OFDM-SNM in placing the active subcarriers in positions where the resultant system provides minimum levels of ICI and/or PAPR.
- SNM module enables the provision of high throughput, especially at low-order modulation. IM, on the other hand, promises EE. The proposed hybrid scheme can, therefore, deliver both simultaneously for certain applications, such as IoT applications.

The remainder of this paper is prepared as follows. The proposed OFDM-HNIM scheme is explained in Section II. We provide a performance evaluation of the proposed scheme in terms of SE, average bit error probability (ABEP), EE, and computational complexity in Section III. Section IV presents the simulation results and comparisons between the proposed hybrid scheme and its competitive schemes. Finally, Section V provides concluding remarks.[1]

[1]Notation: Matrices and column vectors are represented by bold, capital and lowercase letters, respectively. $E(.)$, $(.)^T$, $(.)^H$, $\lfloor . \rfloor$ and $|.|$ represent expectation, transposition, Hermitian transposition, floor, and absolute value operations, respectively. $\det(\mathbf{A})$ denotes the determinant of $\mathbf{A}$. $\binom{n}{k} = \frac{n!}{k!(n-k)!}$ represents the binomial coefficient. $Q(.)$ represents the Q-function. $\sim \mathcal{O}(.)$ denotes the complexity order of a technique. $\mathcal{S}$ represents the complex signal constellation of size M.

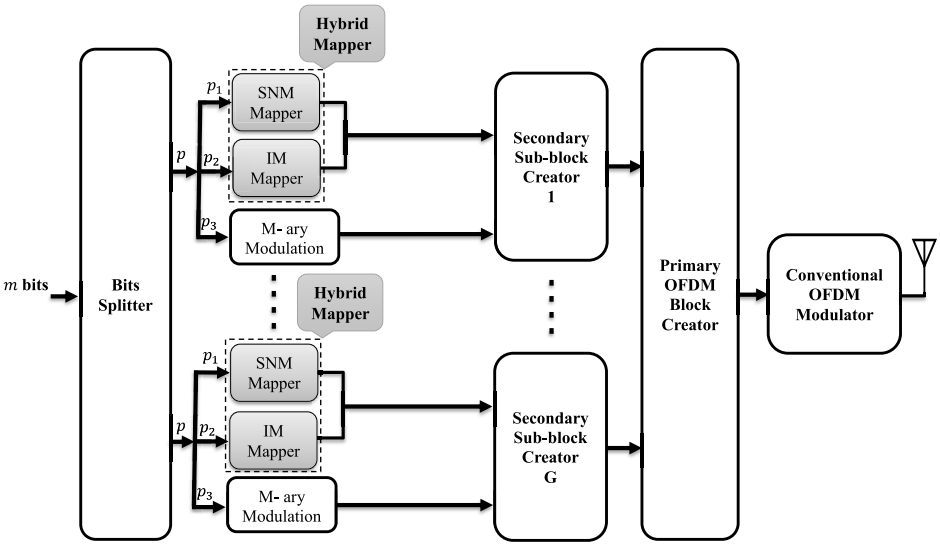

FIGURE 1. The proposed OFDM-HNIM transmitter structure.

II. PROPOSED HYBRID SCHEME

The block diagram of the proposed OFDM-HNIM transmitter is displayed in Fig. 1. The m incoming bits are partitioned into G subblocks using bits splitter, each subblock of length L subcarriers contains $p = p_1 + p_2 + p_3$ bits. The non-conventional bits, p_1 and p_2, represent the bits conveyed by the SNM and IM modulators, respectively. In each subblock, the SNM and IM mappers can be ordered arbitrary since the hybrid mapper combines both mappings without considering their order. For convenient representation of the basic OFDM-HNIM system model, we represent the SNM bits by p_1, which are utilized by the SNM mapper to specify the number of active OFDM subcarriers for each subblock, and p_2 bits, referred to IM bits, are exploited by the IM mapper to specify the indices of active subcarriers within each subblock. Then, the combined SNM and IM mapping performed by the hybrid mapper determines the subcarrier activation pattern (SAP) using a proper mapping technique.

The full set of N_F subcarriers that constitutes the OFDM block can be represented by $\mathbb{B} = \{1, 2, \ldots, N_F\}$. Based on the hybrid mapper, specific active subcarriers in each subblock are selected from $\mathbb{B}$, which can be represented by the subset $\mathbb{B}_g \subset \mathbb{B}$, where $g = 1, 2, \ldots, G$ is the index of the subblock. The number of active subcarriers in the g-th subblock ($I(g)$) is an **index and number-dependent variable** that represents the cardinality of $\mathbb{B}_g$ (i.e. $I(g) = |\mathbb{B}_g|$).

The conventional $p_3 = I(g)\log_2(M)$ bits of the g-th subblock correspond to M-ary conventional constellation symbols carried over $I(g)$ active subcarriers. Table 1 presents a bits-to-SAP mapping for small values of $L = 4$ with fixed length of $p_1 = p_2 = \log_2(L) = 2$ bits to simplify the system-level design. The SAP for the g-th subblock can be written as follows:

$$\mathbf{c_g} = \left[c(1)\ c(2)\ \cdots\ c(L)\right]^T, \tag{1}$$

where $c(i) \in \{0, 1\}$ for $i = 1, 2, \cdots, L$.

TABLE 1. Look-up table of the proposed OFDM-HNIM scheme with $p_1 = p_2 = 2$ bits.

g	p_1	p_2	$\mathbf{c_g}$	$I(g)$
1	[0 0]	[0 0]	$[1\,0\,0\,0]^T$	1
2	[0 0]	[0 1]	$[0\,1\,0\,0]^T$	1
3	[0 0]	[1 0]	$[0\,0\,1\,0]^T$	1
4	[0 0]	[1 1]	$[0\,0\,0\,1]^T$	1
5	[0 1]	[0 0]	$[1\,1\,0\,0]^T$	2
6	[0 1]	[0 1]	$[1\,0\,1\,0]^T$	2
7	[0 1]	[1 0]	$[1\,0\,0\,1]^T$	2
8	[0 1]	[1 1]	$[0\,1\,0\,1]^T$	2
9	[1 0]	[0 0]	$[1\,1\,1\,0]^T$	3
10	[1 0]	[0 1]	$[1\,0\,1\,1]^T$	3
11	[1 0]	[1 0]	$[1\,1\,0\,1]^T$	3
12	[1 0]	[1 1]	$[0\,1\,1\,1]^T$	3
13	[1 1]	[0 0]	$[0\,0\,0\,0]^T$	0
14	[1 1]	[0 1]	$[0\,0\,1\,1]^T$	2
15	[1 1]	[1 0]	$[0\,1\,1\,0]^T$	2
16	[1 1]	[1 1]	$[1\,1\,1\,1]^T$	4

As shown in Table 1, a subcarrier in a given index of $\mathbf{c_g}$ is activated with an equal probability of 1/2. The presented codebook ($\mathbf{c_g}$) in Table 1 looks like a classical codebook generated in binary order; however, they are different in the sense that the direct binary mapping does not provide flexibility, whereas, the proposed scheme is an adaptive and flexible transmission technique, whose mapping blocks can be employed based on the requirements of the used application. For example, SNM and IM mapping blocks are proper mappers for throughput-aware, especially at low-order modulation, and EE-aware applications, respectively [7]. Therefore, the proposed hybrid mapper is appropriate for both throughput-aware and EE-aware applications.

It should be noted that there would be similar SAP when $g = 13, 14, 15, 16$ as expected from their SNM mapping, due to setting a fixed length of p_2 data code. To solve this ambiguity in mapping, extra bits could be transmitted to a receiver to differentiate between these exceptional cases.

However, this solution is not spectrally efficient due to sending additional non-data bits. Moreover, the expected SNM mapping leads to a nonuniform subcarrier activation, which results in unfair protection of transmitted bits, thus hindering the OFDM-SNM and OFDM-IM relevant schemes from attaining their ultimate error performance.

The problem of unbalanced activation of subcarriers in the OFDM-SNM and OFDM-IM schemes is avoided in the proposed mapping process, which is represented in Table 1, by having an equiprobable probability of subcarrier activation without relying on the channel status [26]. To avoid ambiguity and extra bits signaling at the ML detector as well as satisfying the equiprobable subcarrier activation (ESA) requirement [26], the aforementioned exceptional cases are assigned unique SAPs where their corresponding $I(g)$ values are mostly different from their expected SNM mapping.

However, the zero-active subcarrier dilemma, where all subcarriers are switched off and their corresponding data symbols cannot be transmitted, can be seen in Table 1 at $g = 13$, which corresponds to $\mathbf{c_g} = [0\,0\,0\,0]^T$. This dilemma could lead to difficulty in higher layer design, especially the synchronization process, which is the key for OFDM-based systems to reduce ICI and/or inter symbol interference (ISI) [12], [27]. One efficient solution to such a dilemma could be done by exploiting the lexicographic ordering principle and implementing the codebook optimization method as in [28], where the codebooks are optimized in such a way that the subcarriers are activated based on their corresponding instantaneous CSI. The novel codebook design in [28] does not involve optimizing the power usage, unlike the forward error correction method that introduces more computational complexity at the receiver [29].

As shown in Table 1, the equally probable bit sequence enables easier detection and flexible designs of higher layer protocols unlike the dual-mode transmission protocol [27], where the bit sequence of variable length is modulated. Control signaling is not required in [28] unlike the method in [30] where the always-active control subcarrier used for control signaling transmission. Therefore, the lexicographic-based codebook design in [28] provides an efficient solution to the observed dilemma as compared to the existing solutions [27], [29], [30]. In this paper, we focus on the basic idea and system model of the proposed OFDM-HNIM, whereas employing the novel design in [28] to the proposed scheme could be considered as a future work for improving the OFDM-HNIM system.[2]

By considering the SAP ($\mathbf{c_g}$) for the g-th subblock, the OFDM subblock can be formed as

$$\mathbf{x_F^g} = \left[x_F^g(1)\; x_F^g(2)\; \cdots\; x_F^g(L)\right]^T, \tag{2}$$

where $x_F^g(i) \in \{0, \mathcal{S}\}$ for $i = 1, 2, \cdots, L$.

The OFDM block of N_F subcarriers is built based on the chain of G subblocks and given as

$$\mathbf{x_F} = \left[x_F(1)\; x_F(2)\; \cdots\; x_F(N_F)\right]^T, \tag{3}$$

where $x_F(k) \in \{0, \mathcal{S}\}$ for $k = 1, 2, \cdots, N_F$.

The remaining steps are done as in the classical OFDM system. By performing N_F-inverse fast Fourier transform (IFFT) to $\mathbf{x_F}$, the output vector is $\mathbf{x_t}$ with dimension $N_F \times 1$. To combat ISI effects, cyclic prefix (CP), of length N_{CP} longer than the channel impulse response (CIR) length v, is appended to the beginning of $\mathbf{x_t}$, the resultant is the transmitted signal represented by

$$\mathbf{x_{CP}} = \left[\mathbf{x_t}(N_F - N_{CP} + 1 : N_F)\; \mathbf{x_t}\right]^T, \tag{4}$$

It is assumed that $\mathbf{x_{CP}}$ passes to a slowly time-varying multipath Rayleigh fading channel modeled by a CIR $\mathbf{h_t} = [h_t(1)\, h_t(2)\; \cdots\; h_t(v)]^T$, whose elements (i.e. $h_t(\sigma)$, $1 \leq \sigma \leq v$) are a circularly symmetric complex Gaussian random variable with the distribution $\mathcal{CN}(0, \frac{1}{v})$ [12]. Then, this channel-impaired received signal is contaminated with additive white Gaussian noise (AWGN) with noise variance of $N_{o,T}$ in the time domain.

The receiver part of the proposed OFDM-HNIM system is the reversal of the transmitter part, which includes CP removal, FFT processing, hybrid demapping, and detection. The frequency-domain received signal vector of dimension $N_F \times 1$ after taking off CP from the received signal and applying FFT can be written as

$$\mathbf{y_F} = \mathbf{X_F h_F} + \mathbf{n_F}, \tag{5}$$

where $\mathbf{X_F}$ is an $N_F \times N_F$ diagonal matrix whose prime-diagonal elements are denoted by $x_F(1)$, $x_F(2)$,..., $x_F(N_F)$. $\mathbf{h_F}$ is the $N_F \times 1$ frequency-domain channel vector following the distribution of $\mathcal{CN}(0, \mathbf{I_{N_F}})$, where $\mathbf{I_{N_F}}$ denotes the identity matrix with dimension $N_F \times N_F$. It should be noted that $\mathbf{h_F} = \mathbf{W_{N_F} h_t^0}$, where $\mathbf{W_{N_F}}$ is the N_F-point discrete Fourier transform (DFT) with $\mathbf{W_{N_F}^H W_{N_F}} = N_F \mathbf{I_{N_F}}$, and $\mathbf{h_t^0}$ is the zero-padded version of the vector $\mathbf{h_t}$ with length N_F (i.e. $\mathbf{h_t^0} = [\mathbf{h_t}, 0, ..., 0]^T$) [12]. $\mathbf{n_F} \sim \mathcal{CN}(0, N_{o,F})$ is the AWGN vector in the frequency domain with zero-mean complex Gaussian distribution of variance $N_{o,F}$. Subsequently, a frequency domain equalizer of one tap is utilized to properly compensate for the frequency selectivity of the multipath channel as $\mathbf{y_{eq}} = \mathbf{y_F}/\mathbf{h_F}$. Then, a detector is employed to extract the SAP.

The remaining steps of the OFDM-HNIM receiver are related to the demapping process. More precisely, the bits conveyed by the index and number of activated subcarriers for each subblock are estimated based on the obtained SAP using the hybrid demapper. To regenerate p_1 and p_2, a mapping (look-up) table similar to Table 1 is used at the receiver, but in a reverse operation to that performed at the transmitter. Then, symbols detection is done based on the received SAP of each subblock. Finally, the detected bits from the hybrid demapping and conventional quadrature amplitude modulation (QAM) detection are combined to give the subblock bits.

[2]In this paper, our main focus is on introducing a new physical layer transmission scheme. The usage of the proposed modulation scheme at the upper layers is out of this paper scope.

By performing similar operations for all subblocks, the data sequence is recovered for the whole OFDM block. Different detectors, including the optimal ML, ML-based, and LLR, which can be used in this process, are explained below.

In the proposed hybrid scheme, the detection of the number and position of active subcarriers as well as the conventional QAM symbols can be performed subblock by subblock without introducing any extra performance loss since the encoding processes for all subblocks are independent. We could employ the ML detector in each subblock to jointly estimate its active subcarriers and traditional symbols as follows:

$$(\hat{\mathbf{s}_g}, \hat{\mathbb{B}}_g) = \arg\min_{\mathbf{s_g}, \mathbb{B}_g} ||\mathbf{y_F^g} - \mathbf{x_F^g}\mathbf{h_F^g}||^2, \tag{6}$$

where $\mathbf{s_g}$ and $\hat{\mathbf{s}_g}$ represent the conventional transmitted and estimated symbols conveyed by the active subcarriers of the g-th subblock, respectively, $\mathbb{B}_g$ and $\hat{\mathbb{B}}_g$ are the set of active subcarriers of the g-th subblock specified by the transmitter and the ML receiver, respectively.

This work studies two different low-complexity approaches for ML-based detection, namely, perfect subcarrier activation pattern estimation (PSAPE), and imperfect SAP estimation (ISAPE). The former ignores the errors due to the incorrect detection of received SAP's subcarriers, while the latter is prone to errors. Particularly, in the case of correct detection of SAP, p_1 and p_2 are detected correctly, while the detection of p_3 is not certain, but depends on the quality of QAM detection. However, in the case of incorrect SAP detection, all subblock bits are erroneous due to the demodulation of some unmodulated subcarriers.

For further reduction in the computational complexity of the proposed OFDM-HNIM scheme, an LLR detector is employed with logarithmic ratios $\lambda(\alpha)$, where $\alpha = 1, 2, \cdots, N_F$, is calculated for the OFDM block, assuming BPSK modulation is used for simplification [12].

$$\lambda(\alpha) = \max(a, b) + \ln(1 + \exp(-|b - a|)) + \frac{\left|\mathbf{y_F^g}(\alpha)\right|^2}{N_{o,F}}, \tag{7}$$

where

$$a = -\frac{\left|\mathbf{y_F^g}(\alpha) - \mathbf{h_F^g}(\alpha)\right|^2}{N_{o,F}}, \tag{8}$$

and

$$b = -\frac{\left|\mathbf{y_F^g}(\alpha) + \mathbf{h_F^g}(\alpha)\right|^2}{N_{o,F}}. \tag{9}$$

The subcarrier with a larger logarithmic ratio implies that it is more probable that this subcarrier carries a constellation symbol. The proposed LLR detector decides on specific active subcarriers that have maximum LLR values. Then, these selected active subcarriers map to p_1 and p_2 bits and the symbols carried over these active subcarriers would be demodulated to acquire the p_3 bits.

III. PERFORMANCE EVALUATION OF THE PROPOSED HYBRID SCHEME

Here, the evaluation of the hybrid system performance is performed based on key metrics such as spectral efficiency, average bit error probability, energy efficiency, and computational complexity.

A. SPECTRAL EFFICIENCY

The achievable rate of the proposed OFDM-HNIM scheme can be calculated based on the mutual information between the channel input and the channel output averaged over the subcarriers [31]. Because the data formation in OFDM-HNIM is performed in a subblock level, whose structure is repeated for all the other consecutive subblocks, the performance evaluation is performed on a subblock basis while considering that the subblocks experience independent, different channel realizations. Therefore, the mutual information over the OFDM block should be calculated for each subblock as shown in (10), which presents the achievable rate of the OFDM-HNIM scheme,

$$R_h = \frac{\mathrm{I}(\mathbf{x_F^g})}{L} = \frac{\mathrm{H}(\mathbf{x_F^g})}{L} + \frac{\mathrm{H}(\mathbf{x_F^g}|\mathbf{y_F^g})}{L}, \tag{10}$$

where $\mathrm{I}(\mathbf{x_F^g})$ represents the mutual information of the channel input of the g-th subblock ($\mathbf{x_F^g}$), $\mathrm{H}(\mathbf{x_F^g})$ is the marginal entropy of $\mathbf{x_F^g}$ and $\mathrm{H}(\mathbf{x_F^g}|\mathbf{y_F^g})$ is the conditional entropy of $\mathbf{x_F^g}$ and the channel output of the g-th subblock ($\mathbf{y_F^g}$).

The achievable rate formula in (10) can be written in terms of probability density functions (PDFs) of the channel input, channel, and channel output as follows [32]:

$$R_h = \eta_h - \frac{1}{2^p L}\sum_{j=1}^{2^p} E_{\mathbf{h_F^g}}\left\{\int f(\mathbf{y_F^g}|\mathbf{x_F}^{g(j)}, \mathbf{h_F^g}) \times \log_2\left(\frac{f(\mathbf{x_F}^{g(j)}, \mathbf{y_F^g}|\mathbf{h_F^g})}{f(\mathbf{y_F^g}|\mathbf{h_F^g})}\right) d\mathbf{y_F^g}\right\}, \tag{11}$$

where $f(\mathbf{y_F^g}|\mathbf{h_F^g}) = \frac{1}{2^p}\sum_{j=1}^{2^p} f(\mathbf{y_F^g}|\mathbf{x_F}^{g(j)}, \mathbf{h_F^g})$, and $\mathbf{x_F}^{g(j)}$ is the j-th realization of $\mathbf{x_F^g}$.

Furthermore, (11) can be simplified to the following in the analogy with [31], [32]:

$$R_h \approx \eta_h - \frac{1}{2^p L}\sum_{j=1}^{2^p}\log_2\sum_{w=1}^{2^p}\frac{1}{det(\mathbf{I_L} + \mathbf{K_L}\mathbf{U}_{j,w})}, \tag{12}$$

where η_h is the SE of the proposed hybrid scheme, and it can be found in (13), $\mathbf{K_L} = E[\mathbf{h_F^g}(\mathbf{h_F^g})^H]$ is the covariance matrix of $\mathbf{h_F^g}$, $\mathbf{I_L}$ represents the identity matrix with dimensions $L \times L$, and $\mathbf{U}_{j,w} = \frac{(\mathbf{x_F}^{g(j)} - \mathbf{x_F}^{g(w)})^H(\mathbf{x_F}^{g(j)} - \mathbf{x_F}^{g(w)})}{2N_{o,F}}$. This analytical result will be verified by simulation as well.

The SE of the proposed OFDM-HNIM scheme is:

$$\eta_h = \frac{\sum_{g=1}^{G}\left(\log_2(L) + \left\lfloor \log_2\binom{L}{I(g)}\right\rfloor + I(g)\log_2(M)\right)}{N_F + N_{CP}}. \tag{13}$$

TABLE 2. SE of the featured OFDM-based modulation schemes with BPSK.

OFDM modulation option	L	$G\,p_1$	$G\,p_2$	$G\,p_3$	$G\,p$	SE gain
Proposed OFDM-HNIM	4	32	32	32	96	1.333
	8	24	24	216	264	3.6667
OFDM-SNM [13]	4	32	40	N/A	72	1
	8	24	36	N/A	60	0.8333
OFDM-IM [12]	4	32	32	N/A	64	0.8889
	8	24	24	N/A	48	0.6667
Conventional OFDM	4	N/A	N/A	N/A	72	1
	8	N/A	N/A	N/A	72	1

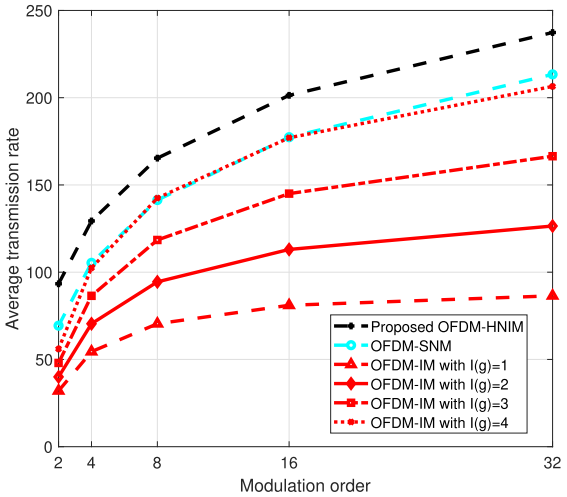

FIGURE 2. Average transmission rate measured in terms of the total number of transmitted bits per OFDM symbol with 64 subcarriers for the featured OFDM-based modulation options as a function of *M* when the subblock size (*L*) is set to 8.

Because two parts of the incoming bits are used for non-conventional mapping in the hybrid scheme compared to only one part in the OFDM-SNM and OFDM-IM schemes, the hybrid scheme improves the SE over the OFDM-IM and OFDM-SNM transmission schemes. For example, Table 2 shows the SE of the proposed hybrid scheme and its competitive schemes including OFDM-SNM, OFDM-IM, and conventional OFDM, assuming $N_F = 64$ with $N_{CP} = 8$, and BPSK modulation is employed.[3] For convenient comparisons, we consider a fixed length of p_2 bits that enter the IM mapper of the OFDM-HNIM scheme. Also, we set the subblock size (L) to either 4 ($G = N_F/L = 64/4 = 16$), or 8 ($G = 64/8 = 8$). For the system settings shown in Table 2, the proposed hybrid scheme outperforms its counterparts in terms of SE. Moreover, the SE becomes much more significant in the hybrid scheme as the subblock length increases. This SE trend cannot be achieved by the conventional OFDM-SNM and OFDM-IM schemes, in which SE is degraded as subblock size rises.

Fig. 2 shows the number of transmitted bits per OFDM symbol with 64 subcarriers for the featured OFDM-based modulation options at a fixed subblock size of 8. It can be observed from Fig. 2 that the OFDM-HNIM scheme outperforms the conventional OFDM-SNM and OFDM-IM schemes at different modulation orders.

[3]The phrase N/A, as shown in Table 2, refers to not applicable.

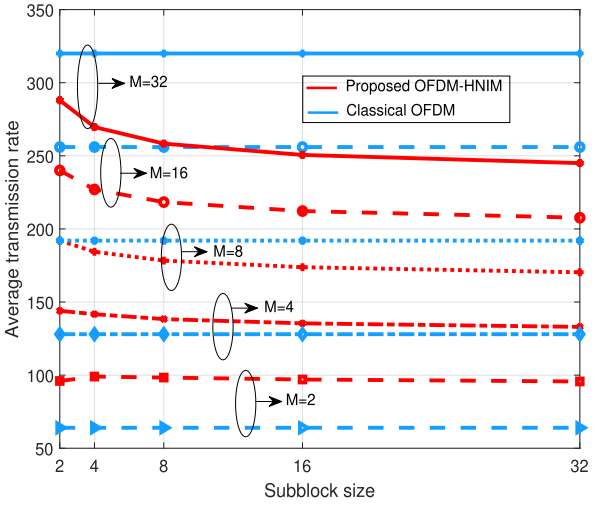

FIGURE 3. Average transmission rate measured in terms of the total number of transmitted bits per OFDM symbol with 64 subcarriers for the proposed hybrid scheme (OFDM-HNIM) and plain OFDM as a function of the subblock size (*L*).

Mathematically, we can deduce the values of M and L that satisfy the condition where the SE of the proposed scheme improves over that of the conventional OFDM. The SE of the hybrid scheme can be calculated from (13) with an average number of active subcarriers of $I_{avg} = \left\lfloor \frac{L+1}{2} \right\rfloor$ over the OFDM subblock:

$$\bar{\eta}_h = \frac{N_F \left(\log_2(L) + \left\lfloor \log_2 \binom{L}{I_{avg}} \right\rfloor + I_{avg} \log_2(M) \right)}{L(N_F + N_{CP})}. \quad (14)$$

By comparing (14) to the SE of the conventional OFDM, which is represented by

$$\bar{\eta}_{OFDM} = \frac{N_F \log_2(M)}{N_F + N_{CP}}, \quad (15)$$

we can observe the trend in the SE for the hybrid scheme and conventional OFDM as M and L vary. Then, we can set the inequality that results from considering the SE of the hybrid scheme greater than that of the conventional OFDM as follows:

$$\log_2(L) + \left\lfloor \log_2 \binom{L}{I_{avg}} \right\rfloor + I_{avg} \log_2(M) \geq L \log_2(M). \quad (16)$$

Fig. 3 shows that the average transmission rate per OFDM symbol with 64 subcarriers for the conventional OFDM does not depend on the subblock size since subblock-based mapping is not employed by the plain OFDM. However, the hybrid scheme outperforms the plain OFDM at low modulation orders, specifically when $M = 2$ or $M = 4$, for different subblock sizes. However, as M increases, it is less likely that the proposed scheme has a higher average transmission rate than the conventional OFDM, and this rate of degradation also increases as subblock size increases. This happens because of having more probable bits experience deep fading as subblock size increases and it becomes difficult for the receiver to detect these bits affected by the deep fade.

B. AVERAGE BIT ERROR PROBABILITY

The whole block of the hybrid scheme should be detected based on the transmission bits that are conveyed in the number and index of activated subcarriers and the conventional constellation symbols [27]. The block error rate (BLER) is computed first, and then the average BER is calculated based on the average BLER [28], [33]. The BLER is expressed in terms of pairwise error probability (PEP). The PEP is calculated in two steps; first, the conditional PEP is calculated by considering the effect of the channel ($\mathbf{h_t}$), then the unconditional PEP is computed by getting rid of the channel effect. The conditional PEP can be represented using the Q-function [34]

$$P(\mathbf{c_g} \longrightarrow \hat{\mathbf{c}}_{\hat{\mathbf{g}}}|\mathbf{h_t}) = Q\left(\sqrt{\frac{P_t}{N_{o,F}}||\mathbf{h_t}(\frac{\mathbf{c_g}}{\sqrt{I(g)}} - \frac{\hat{\mathbf{c}}_{\hat{\mathbf{g}}}}{\sqrt{I(\hat{g})}})||^2}\right), \tag{17}$$

where P_t represents the total transmit power, $I(g)$ and $I(\hat{g})$ represent the number of active subcarriers in the g-th transmitted and $\hat{g}$-th detected, received subblock, respectively, $\mathbf{c_g}$ and $\hat{\mathbf{c}}_{\hat{\mathbf{g}}}$ are the transmitted and detected SAPs of the g-th and $\hat{g}$-th subblocks, respectively. The conditional PEP shown in (17) can be approximated by using the exponential approximation of the Q-function as [35], [36]

$$Q(x) \approx \sum_{j=1}^{2} \rho_j \exp(-q_j x^2), \tag{18}$$

where $\rho_1 = 1/12$ and $\rho_2 = 1/4$, $q_1 = 1/2$ and $q_2 = 2/3$. The new formula of the conditional PEP becomes [25]

$$P(\mathbf{c_g} \longrightarrow \hat{\mathbf{c}}_{\hat{\mathbf{g}}}|\mathbf{h_t}) = \sum_{j=1}^{2} \rho_j \prod_{l=1}^{L} \exp\left(\frac{-q_j P_t}{N_{o,F}} V(l)\Delta(l, g, \hat{g})\right), \tag{19}$$

where $V(l) = |h_t(l)|^2$ and $\Delta(l, g, \hat{g}) = \left|\frac{\mathbf{c_g}(l)}{\sqrt{I(g)}} - \frac{\hat{\mathbf{c}}_{\hat{\mathbf{g}}}(l)}{\sqrt{I(\hat{g})}}\right|^2$.

The unconditional PEP can be found by averaging the conditional PEP over the channel as [37], [38]

$$P(\mathbf{c_g} \longrightarrow \hat{\mathbf{c}}_{\hat{\mathbf{g}}}) = \sum_{\hat{\mathbf{c}}_{\hat{\mathbf{g}}} \neq \mathbf{c_g}} E_{\mathbf{h_t}}\{P(\mathbf{c_g} \longrightarrow \hat{\mathbf{c}}_{\hat{\mathbf{g}}})|\mathbf{h_t})\}. \tag{20}$$

Assuming equiprobable information bits, the upper bound of ABEP of the hybrid system could be obtained as [12], [39]

$$P_b(E) = \frac{1}{p_g\, n_x} \sum_{g=1}^{G} \sum_{\hat{\mathbf{c}}_{\hat{\mathbf{g}}} \neq \mathbf{c_g}} P(\mathbf{c_g} \longrightarrow \hat{\mathbf{c}}_{\hat{\mathbf{g}}}) e(\mathbf{c_g}, \hat{\mathbf{c}}_{\hat{\mathbf{g}}}), \tag{21}$$

where p_g represents the vector length of the information bits that correspond to the g-th subblock, n_x represents the number of possible realizations of the transmitted sequence, and $e(\mathbf{c_g}, \hat{\mathbf{c}}_{\hat{\mathbf{g}}})$ denotes errors in information bits due to erroneously choosing $\hat{\mathbf{c}}_{\hat{\mathbf{g}}}$ rather than $\mathbf{c_g}$ [12]. This derived theoretical BER result will be verified by simulations as well.

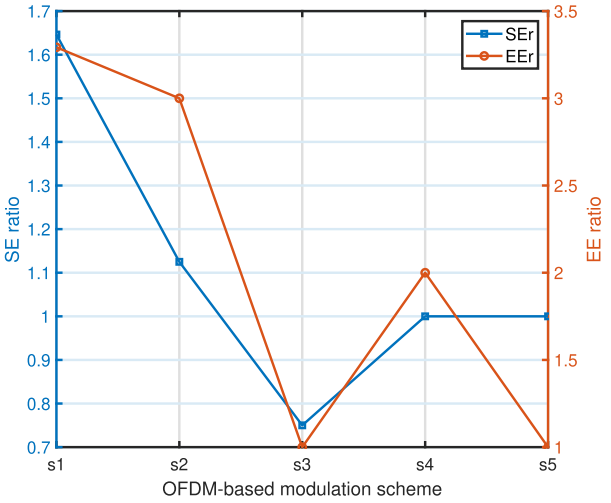

FIGURE 4. The SE and EE ratios of the featured OFDM-based modulation options. The symbols s1, s2, s3, s4, s5 correspond to the proposed OFDM-HNIM scheme, OFDM-SNM, OFDM-IM with $AR = 0.25$, OFDM-IM with $AR = 0.5$, and conventional OFDM, respectively.

C. ENERGY EFFICIENCY

The energy efficiency (EE) implies how efficiently energy is consumed in a given system. The EE of the proposed OFDM-HNIM scheme is analyzed in terms of the energy saving factor (ESF) achieved by not activating all of the available subcarriers in the OFDM block. The evaluation of ESF for the featured schemes is discussed below.

One main aspect of the overall energy saving is the saving in signal transmission [11]. For the considered OFDM-based modulation options, we define the EE based on the ratio of saved energy under a given total transmit power (P_t) in a single OFDM symbol. We assume equiprobable subcarrier activation [26] for a convenient comparison between the proposed OFDM-HNIM scheme and its competitive schemes. Moreover, the average number of active subcarriers is considered in our analysis of EE. The number of activated subcarriers in an OFDM block impacts both SE and EE, and their ratios relation for the traditional OFDM as a reference scheme [40], can be defined as [11]

$$EE_r = \frac{SE_r}{1 - ESF}, \tag{22}$$

where EE_r and SE_r represent the EE and SE ratios of the scheme of interest, and ESF represents the saved energy by activating N_a subcarriers out of N_v available subcarriers

$$ESF = 1 - \frac{N_a}{N_v}. \tag{23}$$

As seen from (23), as N_a decreases, ESF increases and more energy could be saved. Maximizing SE and EE are generally two conflicting objectives as can be seen from (22) [41]. Moreover, the term ($I_{avg} \log_2(M)$) in (14) characterizes the SE and EE trade-off by using high I_{avg} and M values to achieve high SE, more energy needed to be spent to attain such a SE.

For example, the proposed OFDM-HNIM scheme with half of the available subcarriers are activated on average is the

TABLE 3. Complexity comparison between different detectors for the featured OFDM-based modulation schemes.

OFDM modulation option	Detector type	Complexity order
Proposed OFDM-HNIM	Optimal ML	$\sim \mathcal{O}(G\,M^{L/2})$
	PSAPE	$\sim \mathcal{O}(G)$
	ISAPE	$\sim \mathcal{O}(G)$
	LLR	$\sim \mathcal{O}(M)$
OFDM-SNM [13]	ML	$\sim O(L, I(g), M)$
OFDM-IM [12]	Near optimal LLR	$\sim O(M)$
Conventional OFDM	ML	$\sim O(M)$

equivalent case of the OFDM-IM scheme with a subcarrier activation ratio of half ($AR = 0.5$). The energy saving resulting from the OFDM-HNIM and OFDM-IM with $AR = 0.5$ is limited to the half of the OFDM symbol ($ESF = 0.5$). In other words, the active subcarriers of the OFDM-HNIM scheme gain higher power as compared to the individual subcarriers of the classical OFDM under the same transmitted power. Hence, the receiver design of the proposed OFDM-HNIM scheme would only differentiate between the active set with higher power and the inactive set regardless of the exact amplitude and phase of each subcarrier.

It is well-known that the conventional OFDM is not an EE scheme since most of the available subcarriers are usually used for data transmission, which results in very low ESF. Fig. 4 shows the SE_r and EE_r of the featured OFDM modulation schemes under BPSK. It is clear from Fig. 4 that the proposed OFDM-HNIM scheme provides higher SE_r and EE_r as compared to the OFDM-SNM, OFDM-IM with low AR, and the classical OFDM.

D. COMPLEXITY ANALYSIS

The computational complexity performances of the proposed detectors of the OFDM-HNIM scheme are discussed here. The computational complexity of the optimal ML detector of the proposed scheme in terms of complex multiplications is of order $\sim \mathcal{O}(G\,M^{L/2})$ per bit detected in each OFDM block, which becomes impractical for large values of G, L, and M, due to its exponentially increasing complexity.

To compare the computational complexity of the proposed detectors, we consider the average number of calculations per subcarrier as the performance metric. Table 3 presents the complexity comparison results for the featured OFDM-based modulation schemes. As seen in Table 3, the computational complexity of the optimal ML detector is highly susceptible to G, L, and M; however, the complexity of the proposed ML-based detectors is only determined by G , and much lower than the optimal ML detector, and there is much reduction of complexity in order of M by employing LLR detector. Moreover, Table 3 shows the comparison between the detection complexity of the proposed hybrid scheme with that of its counterparts schemes such as OFDM-SNM, OFDM-IM, and plain OFDM. The proposed OFDM-HNIM along with the LLR detector is considered as a simple, not sophisticated scheme with similar complexity order to that in OFDM-IM and conventional OFDM.

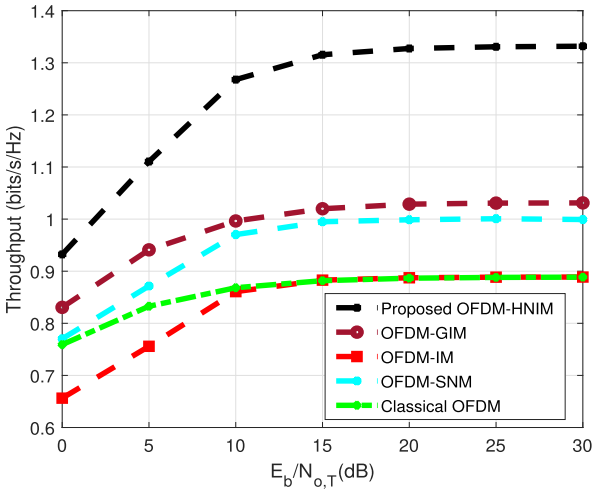

FIGURE 5. Throughput performance over the available OFDM subcarriers of the proposed scheme and its competitive schemes under BPSK.

IV. SIMULATION RESULTS

Throughput, BER, and PAPR performance metrics of the proposed hybrid scheme are compared to those of OFDM-GIM. We assume that the number of allowed active subcarriers of the OFDM-GIM is one, two, or three out of four available subcarriers in each subblock [21]. The proposed scheme is also compared with the OFDM-IM, OFDM-SNM, and conventional OFDM.

It is assumed that FFT size is $N_F = 64$, subblock length is $L = 4$, and $p_1 = p_2 = \log_2(L) = 2$ bits for each subblock. The modulation used in simulations is BPSK. A Rayleigh fading frequency-selective channel with an impulse response of length 9 and normalized power delay profile given by $\boldsymbol{\varrho} = [0.8407, 0, 0, 0.1332, 0, 0.0168, 0.0067, 0, 0.0027]$ mW is considered [42]. We assume here that the CP length (N_{CP}) is longer than the effective CIR, and there is no Doppler effect. For a fair comparison, the same SNR ($E_b/N_{o,T}$) level is assumed for all schemes, where E_b is the bit energy. The number of iterations in the conducted Monte Carlo simulations is 8000. The proposed OFDM-HNIM scheme is evaluated under ideal channel conditions and imperfect channel state information to assess its robustness.

A. PERFORMANCE OF THE PROPOSED OFDM-HNIM SCHEME UNDER IDEAL CHANNEL CONDITIONS

Fig. 5 and Fig. 6 shows the throughput performance of the proposed scheme compared to its competitive schemes under different modulation types. In the conducted simulations, the throughput is calculated by multiplying the SE for a given modulation scheme with BER subtracted from one. The saturation points of the achievable rates or SEs of all the schemes occur at very high SNR. These SE values are dependent on the mapping between incoming bits, SAPs, and conventional symbols.

At a low order modulation (i.e. BPSK), as shown in Fig. 5, the SE of the hybrid scheme is 1.33 bits/s/Hz with SE gain of 0.44, 0.33, and 0.3 compared to OFDM-IM and conventional

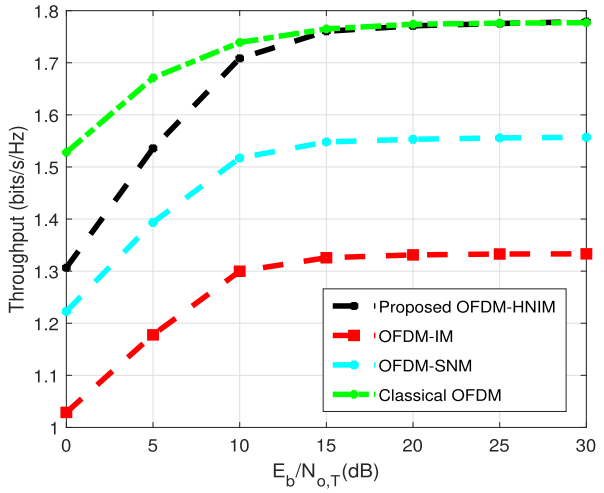

FIGURE 6. Throughput performance over the available OFDM subcarriers of the proposed scheme and its competitive schemes under QPSK.

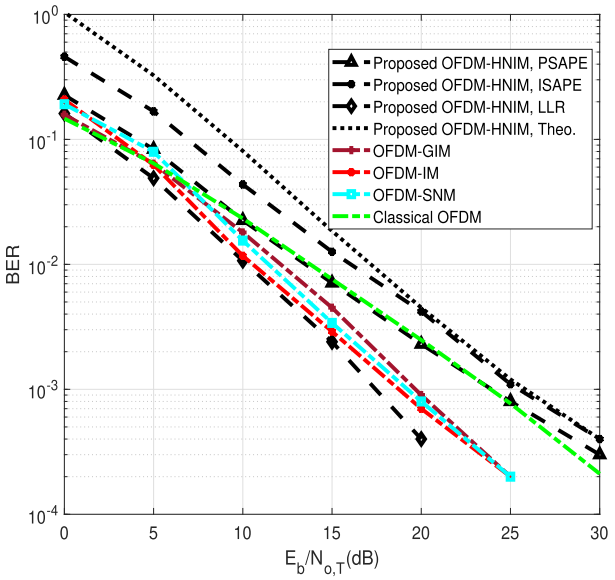

FIGURE 7. BER of the proposed scheme, OFDM-GIM, OFDM-IM, OFDM-SNM, and classical OFDM under frequency-selective Rayleigh channel with BPSK.

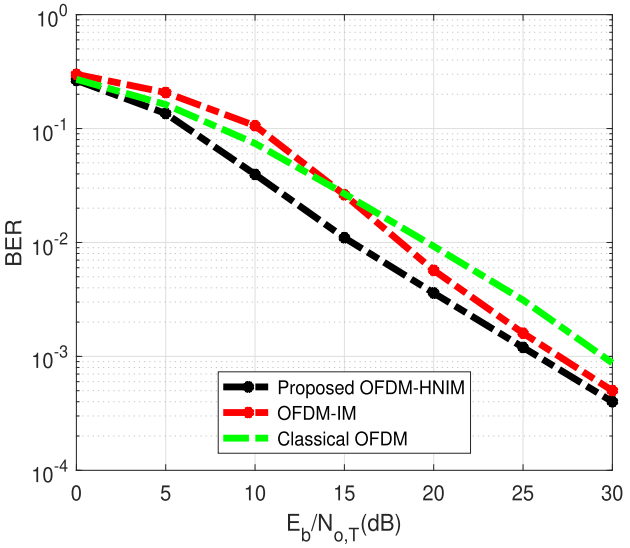

FIGURE 8. BER of the proposed scheme, OFDM-IM, and classical OFDM under frequency-selective Rayleigh channel with SE of 1.78 bits/s/Hz.

OFDM, OFDM-SNM, and OFDM GIM, respectively. The reason behind the superiority of the hybrid scheme over other schemes using BPSK modulation is due to the low noise and interference effects in lower-order modulation as well as the additional information sent by the indices and number of active subcarriers. This shows that OFDM-HNIM provides better SE compared to its OFDM-IM and OFDM-SNM counterparts, where only the indices or numbers of activated subcarriers are exploited to convey additional data bits.

The throughput performances of the featured OFDM-based schemes under quadrature phase shift keying (QPSK) are shown in Fig. 6, where SE superiority of the OFDM-HNIM scheme also seen over conventional OFDM-SNM and OFDM-IM schemes. However, the classical OFDM outperforms the OFDM-HNIM in terms of throughput under QPSK at low SNR values due to the sparse distribution of active subcarriers in the proposed hybrid scheme, OFDM-SNM, and OFDM-IM schemes.

Fig. 7 shows the BER performance of the featured OFDM-based modulation options under BPSK. We assume that the same total power is allocated to the transmitters of the considered schemes, and the original power of the inactive subcarriers evenly reallocated to the active ones. Due to the three different sources of errors that occurred when using the ISAPE-based detector with the hybrid system, its BER performance would be worse than that of the PSAPE detector.

As shown in Fig. 7, using the LLR detector with the proposed OFDM-HNIM scheme provides the best performance in the SNR range of interest. Employing PSAPE and ISAPE detectors, on the other hand, results in non-competitive BER performance, especially in the high SNR region. This is due to the weaker protection offered to the number and index-modulated bits compared to conventionally modulated ones, leaving them prone to a higher number of errors. Moreover, due to the high ratio of number and index-modulated bits, their impact on BER is magnified. Furthermore, Fig. 7 shows reasonable theoretical ABEP results to that using computer simulations as SNR increases, which proves the correctness of the theoretical analysis.

To have a fair comparison between the proposed scheme and its competitive schemes under equivalent SE, their BER performances are simulated under the same SE. Particularly, the BER performance of the proposed scheme is compared to OFDM-IM and conventional OFDM, at equivalent SE of 1.78 bits/s/Hz, as shown in Fig. 8. To attain this SE, the active subcarriers of each subblock of the proposed scheme are modulated by QPSK. While the active subcarriers, of the OFDM-IM and conventional OFDM, are loaded with 8-QAM and QPSK, respectively.

As shown in Fig. 8, the proposed OFDM-HNIM significantly outperforms OFDM-IM and conventional

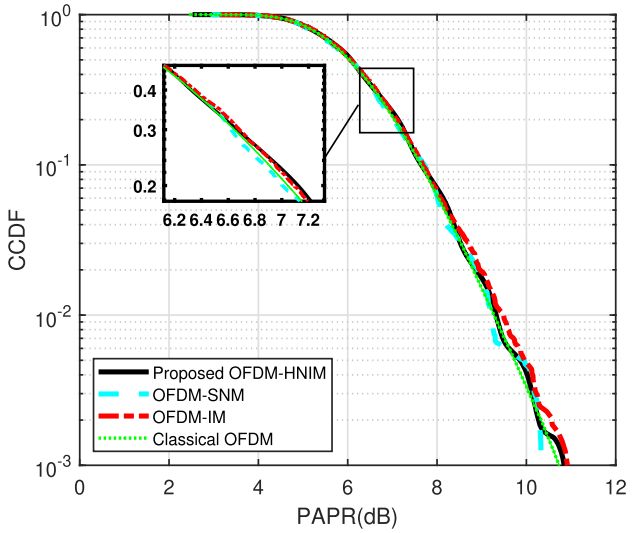

FIGURE 9. PAPR performances of the featured OFDM modulation options.

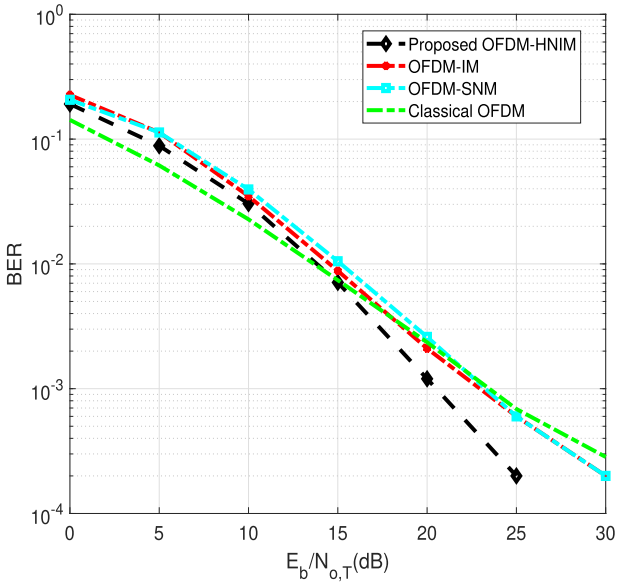

FIGURE 10. BER performance of the proposed OFDM-HNIM scheme, OFDM-IM, OFDM-SNM, and classical OFDM with imperfect CSI with $\beta = 1$, and BPSK.

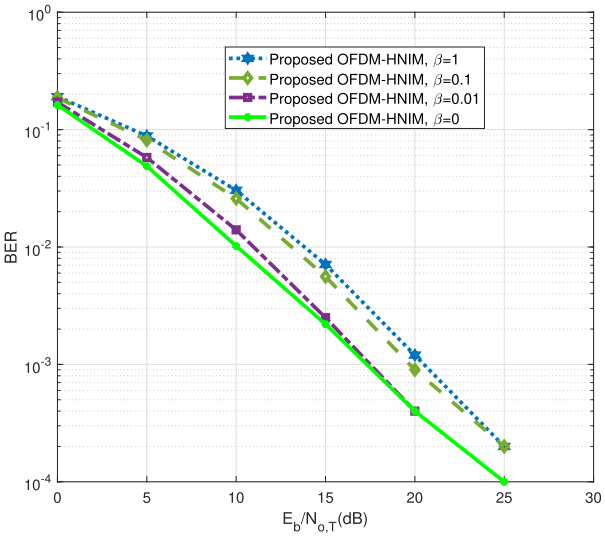

FIGURE 11. The effect of imperfect channel estimation on the proposed OFDM-HNIM scheme.

OFDM schemes in terms of BER under equivalent SE of 1.78 bits/s/Hz. Particularly, the OFDM-HNIM scheme has much better BER performance over OFDM-IM at the low SNR region, but this considerable improvement degrades slightly for high SNR values. The reason behind this SNR-loss in OFDM-IM compared to the hybrid scheme at low SNR values is that the effective power per subcarrier in OFDM-HNIM is more than that of OFDM-IM due to having higher EE. This results in making the sensitivity of OFDM-IM to both noise and interference to achieve the same SE much higher as compared to the OFDM-HNIM scheme.

Fig. 9 presents the complementary cumulative distribution functions (CCDFs) of the PAPR of the proposed OFDM-HNIM scheme compared to its counterparts. Fig. 9 shows that the PAPR performances of these featured OFDM modulation options are high and almost the same as plain OFDM [7], [43]. The reason behind this high PAPR performance of the proposed OFDM-HNIM scheme is the sparsity nature of active subcarriers in OFDM-HNIM, which is also a problem in the conventional OFDM-SNM and OFDM-IM schemes. This inherent feature of having some inactive subcarriers in OFDM-HNIM, OFDM-SNM, and OFDM-IM schemes can be exploited to reduce the PAPR by designing a proper mapping while ensuring that the PAPR level is minimal. The proposed PAPR reduction techniques for conventional OFDM [44] may not be directly applied to non-conventional OFDM modulation schemes such as the OFDM-HNIM scheme. The reason behind this is having unique features and characteristics for different OFDM modulation options [7]. Therefore, we need proper, effective PAPR reduction methods to reduce the PAPR of the proposed OFDM-HNIM scheme, which is left for future works.

B. PERFORMANCE OF THE PROPOSED OFDM-HNIM SCHEME UNDER IMPERFECT CHANNEL ESTIMATION

The subcarrier activation in the proposed scheme, OFDM-SNM, and OFDM-IM schemes is dependent on the non-conventional bits, i.e. index and number bits for the proposed OFDM-HNIM scheme, and index bits for the OFDM-IM scheme. Therefore, channel estimation techniques developed for conventional OFDM cannot be applied directly to these schemes [45]. Some channel estimation methods for OFDM-IM have been proposed in [45] based on its subcarrier activation process. Particularly, pilot symbols are inserted in the frequency domain based on the active subcarriers for tracking the channel variation. After that, the existing interpolation algorithms, such as piecewise linear interpolation (PLI) [46], are applied to estimate the channel frequency response at data symbols. Based on the general principle of subcarrier activation in OFDM-HNIM and OFDM IM, the developed channel esti-

mation techniques for OFDM-IM [45] could be applied to OFDM-HNIM.

It is assumed that the channel estimation process is performed before data transmission. The estimate version of the channel can be represented by an error vector added to the CIR vector ($\mathbf{h_t}$) as

$$\widetilde{\mathbf{h}}_\mathbf{t} = \mathbf{h_t} + \boldsymbol{\epsilon}, \tag{24}$$

where $\boldsymbol{\epsilon} \sim \mathcal{CN}(0, \beta)$ represents the channel estimation error vector, which is independent of $\mathbf{h_t}$. Fig. 10 shows the BER performance of our proposed scheme compared to its counterparts under low channel estimation quality, particularly when $\beta = 1$. It is clearly shown that our scheme is robust against channel estimation errors, especially in the high SNR regime. Moreover, the effect of channel estimation error on the proposed scheme is investigated under different channel estimation qualities with $\beta = 0.01$, $\beta = 0.1$, and $\beta = 1$. For comparison purposes, the performance of the perfect channel estimation case ($\beta = 0$) is also included. Fig. 11 shows that the BER performance gets better as the channel estimation quality enhances (i.e., low values of β). Particularly, the proposed scheme is resistant to channel estimation errors for values of $\beta < 0.01$, and there is 3 dB degradation in BER when $\beta > 0.1$ compared to the perfect channel estimation case. This performance of the proposed scheme under imperfect channel estimation error could be further improved by using the existing algorithms in the literature, such as the algorithm in [47].

V. CONCLUSION

This paper proposes new energy and spectrally efficient multi-carrier transmission scheme named OFDM with hybrid number and index modulation (OFDM-HNIM) that transmits additional information bits by number and index of the active subcarriers along with the conventional signal constellation symbols. The OFDM-SNM and OFDM-IM schemes are combined to harvest both of their advantages. The proposed hybrid scheme has a low-complex transceiver, which has outperformed its competitive schemes in terms of throughput performance under low-order modulation formats such as BPSK and QPSK, but it loses its dominance as the modulation order increases. The proposed hybrid scheme has also outperformed OFDM-IM and classical OFDM in terms of BER under equivalent SE of 1.78 bits/s/Hz. The obtained results prove that our OFDM-HNIM scheme is resilient to channel estimation errors. Moreover, Monte Carlo simulations have been conducted and the obtained results have validated the analysis. Due to having inactive subcarriers within the OFDM symbol of the proposed hybrid scheme, it could be used to reduce interference among subcarriers, and enhance EE by reducing PAPR. Furthermore, it is possible to design and develop much more advanced and effective modulation techniques by integrating the recently introduced subcarrier power modulation concept in [48] and [49] with the proposed hybrid scheme (OFDM-HNIM) to further improve the spectral efficiency performance.

ACKNOWLEDGMENT

This paper is partially supported by the Scientific and Technological Research Council of Turkey (TUBITAK) under Grant 119E392.

REFERENCES

[1] J. G. Andrews, S. Buzzi, W. Choi, S. V. Hanly, A. Lozano, A. C. K. Soong, and J. C. Zhang, "What will 5G be?" *IEEE J. Sel. Areas Commun.*, vol. 32, no. 6, pp. 1065–1082, Jun. 2014.

[2] G. Wunder, P. Jung, M. Kasparick, T. Wild, F. Schaich, Y. Chen, S. Brink, I. Gaspar, N. Michailow, A. Festag, L. Mendes, N. Cassiau, D. Ktenas, M. Dryjanski, S. Pietrzyk, B. Eged, P. Vago, and F. Wiedmann, "5GNOW: Non-orthogonal, asynchronous waveforms for future mobile applications," *IEEE Commun. Mag.*, vol. 52, no. 2, pp. 97–105, Feb. 2014.

[3] A. A. Zaidi, R. Baldemair, H. Tullberg, H. Bjorkegren, L. Sundstrom, J. Medbo, C. Kilinc, and I. Da Silva, "Waveform and numerology to support 5G services and requirements," *IEEE Commun. Mag.*, vol. 54, no. 11, pp. 90–98, Nov. 2016.

[4] Z. E. Ankarali, B. Pekoz, and H. Arslan, "Flexible radio access beyond 5G: A future projection on waveform, numerology, and frame design principles," *IEEE Access*, vol. 5, pp. 18295–18309, 2017.

[5] P. Banelli, S. Buzzi, G. Colavolpe, A. Modenini, F. Rusek, and A. Ugolini, "Modulation formats and waveforms for 5G networks: Who will be the heir of OFDM?: An overview of alternative modulation schemes for improved spectral efficiency," *IEEE Signal Process. Mag.*, vol. 31, no. 6, pp. 80–93, Nov. 2014.

[6] Y. Cai, Z. Qin, F. Cui, G. Y. Li, and J. A. McCann, "Modulation and multiple access for 5G networks," *IEEE Commun. Surveys Tuts.*, vol. 20, no. 1, pp. 629–646, 1st Quart., 2018.

[7] A. M. Jaradat, J. M. Hamamreh, and H. Arslan, "Modulation options for OFDM-based waveforms: Classification, comparison, and future directions," *IEEE Access*, vol. 7, pp. 17263–17278, 2019.

[8] A. Sahin, I. Guvenc, and H. Arslan, "A survey on multicarrier communications: Prototype filters, lattice structures, and implementation aspects," *IEEE Commun. Surveys Tuts.*, vol. 16, no. 3, pp. 1312–1338, 3rd Quart., 2014.

[9] T. Hwang, C. Yang, G. Wu, S. Li, and G. Ye Li, "OFDM and its wireless applications: A survey," *IEEE Trans. Veh. Technol.*, vol. 58, no. 4, pp. 1673–1694, May 2009.

[10] M. Vaezi, Z. Ding, and H. Poor, *Multiple Access Techniques for 5G Wireless Networks and Beyond*. Cham, Switzerland: Springer, 2018.

[11] M. Salah, O. A. Omer, and U. S. Mohammed, "Spectral efficiency enhancement based on sparsely indexed modulation for green radio communication," *IEEE Access*, vol. 7, pp. 31913–31925, 2019.

[12] E. Başar, Ü. Aygölü, E. Panayirci, and H. V. Poor, "Orthogonal frequency division multiplexing with index modulation," *IEEE Trans. Signal Process.*, vol. 61, no. 22, pp. 5536–5549, Nov. 2013.

[13] A. M. Jaradat, J. M. Hamamreh, and H. Arslan, "OFDM with subcarrier number modulation," *IEEE Wireless Commun. Lett.*, vol. 7, no. 6, pp. 914–917, Dec. 2018.

[14] S. Gokceli, E. Basar, M. Wen, and G. Karabulut Kurt, "Practical implementation of index modulation-based waveforms," *IEEE Access*, vol. 5, pp. 25463–25473, 2017.

[15] E. Basar, "Index modulation techniques for 5G wireless networks," *IEEE Commun. Mag.*, vol. 54, no. 7, pp. 168–175, Jul. 2016.

[16] M. Wen, X. Cheng, and L. Yang, *Index Modulation for 5G Wireless Communications*. Cham, Switzerland: Springer, 2016.

[17] E. Basar, M. Wen, R. Mesleh, M. Di Renzo, Y. Xiao, and H. Haas, "Index modulation techniques for next-generation wireless networks," *IEEE Access*, vol. 5, pp. 16693–16746, 2017.

[18] B. Shamasundar, S. Bhat, S. Jacob, and A. Chockalingam, "Multidimensional index modulation in wireless communications," *IEEE Access*, vol. 6, pp. 589–604, 2018.

[19] T. Mao, Q. Wang, Z. Wang, and S. Chen, "Novel index modulation techniques: A survey," *IEEE Commun. Surveys Tuts.*, vol. 21, no. 1, pp. 315–348, 1st Quart., 2019.

[20] X. Cheng, M. Zhang, M. Wen, and L. Yang, "Index modulation for 5G: Striving to do more with less," *IEEE Wireless Commun.*, vol. 25, no. 2, pp. 126–132, Apr. 2018.

[21] R. Fan, Y. J. Yu, and Y. L. Guan, "Generalization of orthogonal frequency division multiplexing with index modulation," *IEEE Trans. Wireless Commun.*, vol. 14, no. 10, pp. 5350–5359, Oct. 2015.

[22] T. Mao, Z. Wang, Q. Wang, S. Chen, and L. Hanzo, "Dual-mode index modulation aided OFDM," *IEEE Access*, vol. 5, pp. 50–60, 2017.
[23] T. Mao, Q. Wang, and Z. Wang, "Generalized dual-mode index modulation aided OFDM," *IEEE Commun. Lett.*, vol. 21, no. 4, pp. 761–764, Apr. 2017.
[24] M. Wen, E. Basar, Q. Li, B. Zheng, and M. Zhang, "Multiple-mode orthogonal frequency division multiplexing with index modulation," *IEEE Trans. Commun.*, vol. 65, no. 9, pp. 3892–3906, Sep. 2017.
[25] S. Dang, G. Ma, B. Shihada, and M.-S. Alouini, "Enhanced orthogonal frequency-division multiplexing with subcarrier number modulation," *IEEE Internet Things J.*, vol. 6, no. 5, pp. 7907–7920, Oct. 2019.
[26] M. Wen, Y. Zhang, J. Li, E. Basar, and F. Chen, "Equiprobable subcarrier activation method for OFDM with index modulation," *IEEE Commun. Lett.*, vol. 20, no. 12, pp. 2386–2389, Dec. 2016.
[27] S. Dang, J. P. Coon, and G. Chen, "Adaptive OFDM with index modulation for two-hop relay-assisted networks," *IEEE Trans. Wireless Commun.*, vol. 17, no. 3, pp. 1923–1936, Mar. 2018.
[28] S. Dang, G. Chen, and J. P. Coon, "Lexicographic codebook design for OFDM with index modulation," *IEEE Trans. Wireless Commun.*, vol. 17, no. 12, pp. 8373–8387, Dec. 2018.
[29] D. Tsonev, S. Sinanovic, and H. Haas, "Enhanced subcarrier index modulation (SIM) OFDM," in *Proc. IEEE GLOBECOM Workshops (GC Wkshps)*, Dec. 2011, pp. 728–732.
[30] Z. Wang, S. Dang, and D. T. Kennedy, "Multi-hop index modulation-aided OFDM with decode-and-forward relaying," *IEEE Access*, vol. 6, pp. 26457–26468, 2018.
[31] M. Wen, X. Cheng, M. Ma, B. Jiao, and H. V. Poor, "On the achievable rate of OFDM with index modulation," *IEEE Trans. Signal Process.*, vol. 64, no. 8, pp. 1919–1932, Apr. 2016.
[32] M. Wen, B. Ye, E. Basar, Q. Li, and F. Ji, "Enhanced orthogonal frequency division multiplexing with index modulation," *IEEE Trans. Wireless Commun.*, vol. 16, no. 7, pp. 4786–4801, Jul. 2017.
[33] S. Dang, J. Li, M. Wen, and S. Mumtaz, "Distributed processing for multi-relay assisted OFDM with index modulation," *IEEE Trans. Wireless Commun.*, vol. 18, no. 2, pp. 1318–1331, Feb. 2019.
[34] H. Jafarkhani, *Space-Time Coding*. Cambridge, U.K.: Cambridge Univ. Press, 2005.
[35] M. Chiani and D. Dardari, "Improved exponential bounds and approximation for the Q-function with application to average error probability computation," in *Proc. Global Telecommun. Conf. (GLOBECOM)*, Nov. 2002, pp. 1399–1402.
[36] M. Chiani, D. Dardari, and M. K. Simon, "New exponential bounds and approximations for the computation of error probability in fading channels," *IEEE Trans. Wireless Commun.*, vol. 24, no. 5, pp. 840–845, May 2003.
[37] Q. Ma, P. Yang, Y. Xiao, H. Bai, and S. Li, "Error probability analysis of OFDM-IM with carrier frequency offset," *IEEE Commun. Lett.*, vol. 20, no. 12, pp. 2434–2437, Dec. 2016.
[38] Q. Li, M. Wen, H. V. Poor, and F. Chen, "Information guided precoding for OFDM," *IEEE Access*, vol. 5, pp. 19644–19656, 2017.
[39] Y. Ko, "A tight upper bound on bit error rate of joint OFDM and multi-carrier index keying," *IEEE Commun. Lett.*, vol. 18, no. 10, pp. 1763–1766, Oct. 2014.
[40] R. Fan, Y. J. Yu, and Y. L. Guan, "Improved orthogonal frequency division multiplexing with generalised index modulation," *IET Commun.*, vol. 10, no. 8, pp. 969–974, May 2016.
[41] G. Li, Z. Xu, C. Xiong, C. Yang, S. Zhang, Y. Chen, and S. Xu, "Energy-efficient wireless communications: Tutorial, survey, and open issues," *IEEE Wireless Commun.*, vol. 18, no. 6, pp. 28–35, Dec. 2011.
[42] Y. Cho, J. Kim, W. Yang, and C. Kang, *MIMO-OFDM Wireless Communications with MATLAB*. Hoboken, NJ, USA: Wiley, 2010.
[43] N. Ishikawa, S. Sugiura, and L. Hanzo, "Subcarrier-index modulation aided OFDM–Will it work?" *IEEE Access*, vol. 4, pp. 2580–2593, 2016.
[44] Y. Rahmatallah and S. Mohan, "Peak-to-average power ratio reduction in OFDM systems: A survey and taxonomy," *IEEE Commun. Surveys Tuts.*, vol. 15, no. 4, pp. 1567–1592, Apr. 2013.
[45] Y. Acar, S. A. Çolak, and E. Basar, "Channel estimation for OFDM-IM systems," *Turkish J. Elect. Eng. Comput. Sci.*, vol. 27, pp. 1908–1921, May 2019.
[46] M.-H. Hsieh and C.-H. Wei, "Channel estimation for OFDM systems based on comb-type pilot arrangement in frequency selective fading channels," *IEEE Trans. Consum. Electron.*, vol. 44, no. 1, pp. 217–225, Feb. 1998.
[47] J. M. Hamamreh, H. M. Furqan, and H. Arslan, "Secure pre-coding and post-coding for OFDM systems along with hardware implementation," in *Proc. 13th Int. Wireless Commun. Mobile Comput. Conf. (IWCMC)*, Jun. 2017, pp. 1338–1343.
[48] A. Hajar, J. M. Hamamreh, M. Abewa, and Y. Belallou, "A spectrally efficient OFDM-based modulation scheme for future wireless systems," in *Proc. Sci. Meeting Elect.-Electron. Biomed. Eng. Comput. Sci. (EBBT)*, Apr. 2019, pp. 1–4.
[49] Y. Belallou, J. M. Hamamreh, and A. Hajar, "OFDM-subcarrier power modulation with two dimensional signal constellations," in *Proc. Innov. Intell. Syst. Appl. Conf. (ASYU)*, Oct. 2019, pp. 1–6.

AHMAD M. JARADAT received the B.Sc. and M.Sc. degrees in communication engineering from Yarmouk University, Irbid, Jordan, in 2013 and 2016, respectively. He is currently pursuing the Ph.D. degree as a member of the Communications, Signal Processing, and Networking Center, Istanbul Medipol University, Turkey. He was an Electronic Engineering Taught Postgraduate Associate with the Electronic Engineering Department, Queen Mary University of London, U.K. His current research interests are in multidimensional modulation techniques, 5G and beyond waveform design and multiple access schemes for future 5G and beyond wireless systems, advanced scheduling for future radio access, as well as signal and channel identification.

JEHAD M. HAMAMREH received the B.Sc. degree in electrical and telecommunication engineering from An-Najah University, Nablus, in 2013, and the Ph.D. degree in electrical-electronics engineering and cyber systems from Istanbul Medipol University, Turkey, in 2018. He was a Researcher at the Department of Electrical and Computer Engineering, Texas A&M University at Qatar. He is currently an Assistant Professor with the Electrical and Electronics Engineering Department, Antalya International (Bilim) University, Turkey. His current research interests include wireless physical and MAC layers security, orthogonal frequency-division multiplexing multiple-input multiple-output systems, advanced waveforms design, multidimensional modulation techniques, and orthogonal/non-orthogonal multiple access schemes for future wireless systems. He is a regular investigator and referee for various scientific journals as well as a TPC member for several international conferences.

HÜSEYIN ARSLAN (Fellow, IEEE) received the B.S. degree from Middle East Technical University, Ankara, Turkey, in 1992, and the M.S. and Ph.D. degrees from Southern Methodist University, Dallas, TX, USA, in 1994 and 1998, respectively.

From 1998 to 2002, he was with the Research Group, Ericsson Inc., NC, USA, where he was involved with several projects related to 2G and 3G wireless communication systems. Since 2002, he has been with the Electrical Engineering Department, University of South Florida, Tampa, FL, USA. He has also been the Dean of the College of Engineering and Natural Sciences, Istanbul Medipol University, since 2014. He was a part-time Consultant for various companies and institutions, including Anritsu Company, Morgan Hill, CA, USA, and The Scientific and Technological Research Council of Turkey (TÜBITAK). His research interests are in physical layer security, mmWave communications, small cells, multicarrier wireless technologies, co-existence issues on heterogeneous networks, aeronautical (high-altitude platform) communications, in vivo channel modeling, and system design. He has served as the Technical Program Committee Chair, Technical Program Committee Member, Session and Symposium Organizer, and Workshop Chair in several IEEE conferences. He is a member of the editorial board for the *IEEE Surveys and Tutorials* and *Sensors* Journal. He has also served as a member of the editorial board for the IEEE TRANSACTIONS ON COMMUNICATIONS, the IEEE TRANSACTIONS ON COGNITIVE COMMUNICATIONS AND NETWORKING, the *Elsevier Physical Communication Journal*, the *Hindawi Journal of Electrical and Computer Engineering*, and the *Wiley Wireless Communication and Mobile Computing Journal*.